

Two solar-mass compact stars: structure, composition, and cooling*

ARMEN SEDRAKIAN[†]

Institute for Theoretical Physics, J. W. Goethe-University,
D-60438 Frankfurt am Main, Germany

I discuss the structure and composition of massive (two solar-mass) neutron stars containing hypernuclear and deconfined quark matter in color superconducting states. Stable configurations featuring such matter are obtained if the equation of state of hadronic matter is stiff above the saturation density, the transition to quark matter takes place at a few times the nuclear saturation density, and the repulsive vector interactions in quark matter are substantial. I also discuss our recent progress in understanding the cooling of massive compact stars with color superconducting quark cores.

PACS numbers: 97.60.Jd, 26.60.Kp, 95.30.Sf

1. Introduction

The heavy-ion collision experiments and compact stars provide mutually complementary channels to address some of the outstanding challenges of the modern particle and nuclear physics. While the energy densities achieved in these experiment are overlapping with the range that must exist in neutron (or more generally compact) stars, their astrophysical studies still provide a window on the properties of dense matter that may be difficult or even impossible to extract otherwise.

The masses of neutron stars are the most sensitive among their integral parameters to the equation of state (hereafter EOS) at high densities. Therefore, pulsar mass measurements provide one of the key experimental constraints on the theory of ultra-dense matter (e.g. Refs. [1, 2]). The masses measured in the pulsar binaries are clustered around the value $1.4 M_{\odot}$ and have been consider as “canonical” for a long time. However,

* Lecture presented at “Three Days on Quarkyonic Island”, HIC for FAIR workshop and XXVIII Max Born Symposium, Wrocław, 19-21 May 2011.

[†] Also Department of Physics, Yerevan State University, Armenia

in recent years mounting evidence emerged in favor of substantially heavier neutron stars with $M \leq 2M_{\odot}$. In particular, the recent discovery of a compact star with a mass of $1.97 M_{\odot}$ measured through the Shapiro delay provides an observationally “clean” lower bound on the maximum mass of a compact star [3].

On the theoretical side it is now well-established that the emergence of new degrees of freedom at high densities softens the EOS of matter. For example, allowing for hyperons can reduce the maximum mass of a sequence of compact stars below the canonical mass of $1.4 M_{\odot}$. A similar reduction may occur if a deconfinement to quark matter takes place, although the softening of the EOS in this case is less dramatic. Thus, the observation of $2M_{\odot}$ mass neutron star is evidence that the ultra-dense matter in neutron stars cannot be soft, *i.e.*, agents that will substantially soften the EOS are potentially excluded. Thus, one of the outstanding challenges in the theory of compact objects is to exploit fully the consequences of this recent observation and, for example, to provide new EOSs that are capable to produce compact objects as massive as the millisecond pulsar J1614-2230.

The cooling of neutron stars provides another channel on the properties of dense matter, which is sensitive to the *composition* of matter and weak interactions therein. The cooling of compact stars can be divided roughly in the following phases. After the initial non-isothermal phase of rapid cooling from temperatures $T \sim 50$ MeV down to 0.1 MeV, a neutron star settles in a thermal quasi-equilibrium state which evolves slowly over the time scales $10^3 - 10^5$ yr down to temperatures $T \sim 0.01$ MeV [4, 5]. In this latter phase the core of the star is isothermal and the temperature gradients are concentrated in the envelope. The cooling rate of the star during this period is determined by the processes of neutrino emission from dense matter, whereby the neutrinos, once produced, leave the star without further interactions. The understanding of the cooling processes that take place during this neutrino radiation era is crucial for the interpretation of the data on surface temperatures of neutron stars. While the long term features of the thermal evolution of neutron stars are insensitive to the non-isothermal cooling stage, the subsequent route in the temperature versus time plane strongly depends on the emissivity of matter during the neutrino-cooling era. Thus, another outstanding question raised by the work of Ref. [3] is how the massive neutron stars, featuring quark matter, cool? The recent observation of the substantial change in the temperature of the neutron star in Cas A poses a further challenge for the theory to explain drastic short-term drop in the temperature of this neutron star [6, 7]. Presently, consistent calculations of the cooling of massive compact stars are virtually absent. First steps in this direction have been taken by a number of groups [8, 9, 10, 11].

A robust feature of cold quark matter is its color superconductivity [12, 13]. Unfortunately, consistent, realistic simulations of cooling of compact stars featuring quark matter are far from trivial because of the complex phase structure of the quark matter at low temperatures and the substantial effort that is needed to understand transport and weak interactions in this matter. The study of neutrino emissivities and thermal conductivity of quark matter in the color superconducting state is in its beginning. In some cases, even crude estimates are not available for these quantities and a pressing requirements for any realistic simulation of thermal evolution of massive compact stars is the development of the knowledge of transport coefficients of these phases.

2. Two solar-mass compact stars with hyperons and color superconducting quarks

The existence of hybrid stars with two solar masses was predicted in a number of models, including those based on the MIT model and NJL models of quark matter and its superconductivity (for reviews see Refs. [12, 13]). Our recent study based on relativistic hypernuclear Lagrangians predicts stiff hypernuclear EOS above saturation density [14]. This enables one to construct stable configurations with masses equal and above the measured 1.97 solar-mass star. The resulting configuration have “exotic” matter in their interiors in the form of hyperons and quark matter, of which the quark matter is color-superconducting in the two-flavor 2SC and/or three-flavor CFL phases.

Here we briefly describe the set-up and main results of Ref. [14]. The nuclear EOS, as is well known, can be constructed starting from a number of principles, see, *e.g.*, [1, 2]. In Ref. [14] a number of relativistic mean-field models were employed to model the low density nuclear matter. As is well-known, these models are fitted to the bulk properties of nuclear matter and hypernuclear data to describe the baryonic octet and its interactions [15, 16]. The underlying Lagrangian is given by

$$\begin{aligned}
\mathcal{L}_B = & \sum_B \bar{\psi}_B [\gamma^\mu (i\partial_\mu - g_{\omega B}\omega_\mu - \frac{1}{2}g_{\rho B}\boldsymbol{\tau} \cdot \boldsymbol{\rho}_\mu) - (m_B - g_{\sigma B}\sigma)]\psi_B \\
& + \frac{1}{2}\partial^\mu\sigma\partial_\mu\sigma - \frac{1}{2}m_\sigma^2\sigma^2 + \frac{1}{2}m_\omega^2\omega^\mu\omega_\mu - \frac{1}{4}\boldsymbol{\rho}^{\mu\nu} \cdot \boldsymbol{\rho}_{\mu\nu} + \frac{1}{2}m_\rho^2\boldsymbol{\rho}^\mu \cdot \boldsymbol{\rho}_\mu \\
& - \frac{1}{3}bm_N(g_{\sigma N}\sigma)^3 - \frac{1}{4}c(g_{\sigma N}\sigma)^4 + \sum_{e^-, \mu^-} \bar{\psi}_\lambda (i\gamma^\mu\partial_\mu - m_\lambda)\psi_\lambda - \frac{1}{4}F^{\mu\nu}F_{\mu\nu},
\end{aligned} \tag{1}$$

where the B -sum is over the baryonic octet $B \equiv p, n, \Lambda, \Sigma^{\pm,0}, \Xi^{-,0}$, ψ_B are

the corresponding Dirac fields, whose interactions are mediated by the σ scalar, ω_μ isoscalar-vector and ρ_μ isovector-vector meson fields. The next-to-last term in Eq. (1) is the Dirac Lagrangian of leptons, $F_{\mu\nu}$ is the energy and momentum tensor of the electromagnetic field. The parameters in Eq. (1) correspond to the NL3 parametrization [17]. Computations were made also with the GM3 parameterization [15], with the result that hyperonic matter cannot be accommodated within this model. The choice of this specific parametrization was made because the nucleonic matter has the stiffest EOS compatible with the nuclear phenomenology. The mean-field pressure of the (hyper)nuclear matter can be obtained from Eq. (1) in the standard fashion [1].

The high-density quark matter was described in Ref. [14] by an NJL Lagrangian, which is extended to include the t' Hooft interaction term ($\propto K$) and the vector interactions ($\propto G_V$) [18]

$$\begin{aligned} \mathcal{L}_Q = & \bar{\psi}(i\gamma^\mu\partial_\mu - \hat{m})\psi + G_V(\bar{\psi}i\gamma^0\psi)^2 + G_S \sum_{a=0}^8 [(\bar{\psi}\lambda_a\psi)^2 + (\bar{\psi}i\gamma_5\lambda_a\psi)^2] \\ & + G_D \sum_{\gamma,c} [\bar{\psi}_\alpha^a i\gamma_5 \epsilon^{\alpha\beta\gamma} \epsilon_{abc} (\psi_C)_\beta^b] [(\bar{\psi}_C)_\rho^r i\gamma_5 \epsilon^{\rho\sigma\gamma} \epsilon_{rsc} \psi_\sigma^8] \\ & - K \{ \det_f [\bar{\psi}(1 + \gamma_5)\psi] + \det_f [\bar{\psi}(1 - \gamma_5)\psi] \}, \end{aligned} \quad (2)$$

where the quark spinor fields ψ_α^a carry color $a = r, g, b$ and flavor ($\alpha = u, d, s$) indices, the matrix of quark current masses is given by $\hat{m} = \text{diag}_f(m_u, m_d, m_s)$, λ_a with $a = 1, \dots, 8$ are the Gell-Mann matrices in the color space, and $\lambda_0 = (2/3)\mathbf{1}_f$. Here G_S and G_D are the couplings in the scalar and di-quark channels. The charge conjugate spinors are defined as $\psi_C = C\bar{\psi}^T$ and $\bar{\psi}_C = \psi^T C$, where $C = i\gamma^2\gamma^0$ is the charge conjugation matrix. The partition function of the system can be evaluated for the Lagrangian (2) neglecting the fluctuations beyond the mean-field [18]. To do so, one linearizes the interaction term keeping the di-quark correlations $\Delta_c \propto (\bar{\psi}_C)_\alpha^a i\gamma_5 \epsilon^{\alpha\beta c} \epsilon_{abc} \psi_\beta^b$ and quark-anti-quark correlations $\sigma_\alpha \propto \bar{\psi}_\alpha^a \psi_\alpha^a$. The pressure derived from (2) reads

$$\begin{aligned} p = & \frac{1}{2\pi^2} \sum_{i=1}^{18} \int_0^\Lambda dk k^2 \left\{ |\epsilon_i| + 2T \ln \left[1 + \exp \left(-\frac{|\epsilon_i|}{T} \right) \right] \right\} + 4K \sigma_u \sigma_d \sigma_s \\ & - \frac{1}{4G_D} \sum_{c=1}^3 |\Delta_c|^2 - 2G_s \sum_{\alpha=1}^3 \sigma_\alpha^2 + \frac{1}{4G_V} (2\omega_0^2 + \phi_0^2) + \sum_{l=e^-, \mu^-} p_l - p_0 - B^*, \end{aligned} \quad (3)$$

where T is the temperature, ϵ_i are the quasiparticle spectra of quarks, $\omega_0 = G_V \langle QM | \psi_u^\dagger \psi_u + \psi_d^\dagger \psi_d | QM \rangle$ and $\phi_0 = 2G_V \langle QM | \psi_s^\dagger \psi_s | QM \rangle$ are the mean

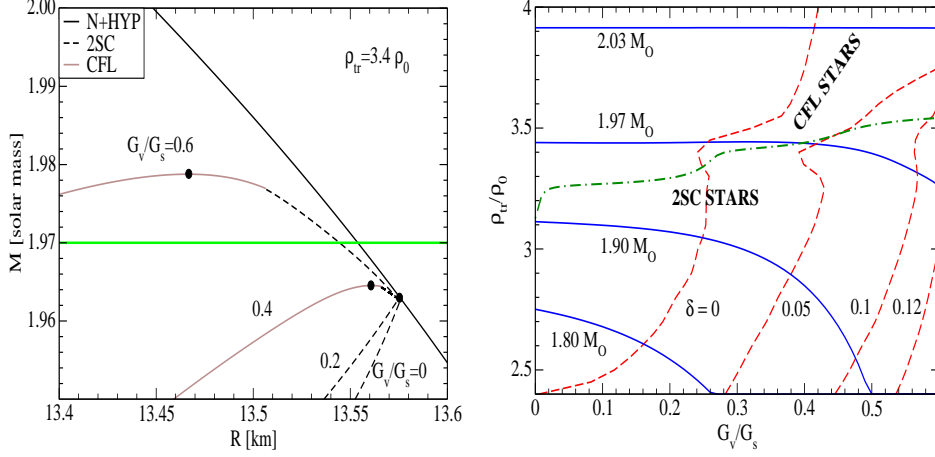


Fig. 1. *Left panel.* Mass vs radius for configurations with quark-hadron transition density $\rho_{tr} = 3.4\rho_0$ for four values of vector coupling $G_V/G_S = 0, 0.2, 0.4, 0.6$. The purely hadronic sequence (i.e. the sequence that includes nucleons and hyperons) is shown by black solid line. The dashed lines and the gray solid lines show the branches where the 2SC and CFL quark phases are present. The filled circles mark the maximum masses of the sequences. The horizontal line shows the largest mass measurement to date [3]. *Right panel.* Properties of the stars as a function the free parameters G_V and ρ_{tr} . The solid lines show the maximum mass configurations realized for the pair of parameters G_V and ρ_{tr} . The dashed curves show the amount of CFL matter in the configurations via the ratio $\delta = R_{CFL}/R$, where R_{CFL} is the radius of the CFL core, R is the star radius. The parameter space to the right from $\delta = 0$ line produces CFL stars. The parameter space below the dashed-dotted 5.1 curve corresponds to stars containing 2SC matter.

field expectation values of the vector mesons ω and ϕ in quark matter, p_l is lepton pressure, p_0 is the vacuum pressure and B^* is an effective bag constant. The quark chemical potentials are modified by the vector fields as follows $\hat{\mu}^* = \text{diag}_f(\mu_u - \omega_0, \mu_d - \omega_0, \mu_s - \phi_0)$. The numerical values of the parameters of the Lagrangians (1) and (2) are quoted in Ref. [14]. The mass-radius relationship for massive stars constructed on the basis of the EOSs described above is shown in the left panel of Fig. 1 together with the largest mass measurement to date $M = 1.97 \pm 0.04 M_\odot$ [3]. Masses above the lower bound on the maximum mass are obtained for purely hadronic stars; this feature is prerequisite for finding similar stars with quark phases. Evidently only for high values of vector coupling G_V one finds stable stars that contain

(at the bifurcation from the hadronic sequence) the 2SC phase, which are followed by stars that additionally contain the CFL phase (for higher central densities). Thus, we find that the stable branch of the sequence contains stars with quark matter in the 2SC and CFL phases.

The right panel of Fig. 1 shows the changes in the masses and composition of compact stars as the parameters of the model G_V and ρ_{tr} are varied. First, it shows the tracks of constant maximum mass compact stars within the parameter space. The decrease of maximum masses with increasing vector coupling reflects the fact that non-zero vector coupling stiffens the EOS. In other words, to obtain a given maximum mass one can admit a small amount of soft quark matter with vanishing vector coupling by choosing a high transition density; the same result is obtained with a low transition density, but strong vector coupling, *i.e.*, a stiffer quark EOS. For low transition densities one finds 2SC matter in stars, which means that weaker vector couplings slightly disfavor 2SC matter. Substantial CFL cores appear in configurations for strong vector coupling and almost independent of the transition density (nearly vertical dashed lines with $\delta \sim 0.1$ in Fig. 1, right panel). Note that for a high transition density there is a direct transition from hyper-nuclear to the CFL phase. For transition densities blow $3.5\rho_0$ a 2SC layer emerges that separates these phases. On the other hand, weak vector couplings and low transition densities produce stars with a 2SC phase only.

3. Thermal evolution of massive stars

New features arise in the cooling behaviour of compact stars with the onset of quark matter in sufficiently high-mass models. The recent development of sequences of stable massive hybrid stars with realistic input EOS [19, 20, 21] allows us to model the thermal evolution of compact stars containing quark cores. These sequences of stable stars permit a transition from hadronic to quark matter in massive stars ($M > 1.85M_\odot$) with the maximal mass of the sequence $\sim 2M_\odot$. In Ref. [11] quark matter of light u and d quarks was assumed in beta equilibrium with electrons. The pairing among the u and d quarks occurs in two channels: the red-green quarks are paired in a condensate with gaps of the order of the electron chemical potential; the blue quarks are paired with (smaller) gaps of order of keV, which is comparable to core temperature during the neutrino-cooling epoch [22, 23, 24]. For the red-green condensate, a parameterization of neutrino emissivity was chosen in terms of the gaplessness parameter $\zeta = \Delta/\delta\mu$, where Δ is the pairing gap in the red-green channel, $\delta\mu$ is the shift in the chemical potentials of the u and d quarks [25]. The magnitude of the gap in the spectrum of blue quarks was treated as a free parameter.

The stellar models were evolved in time, with the input described above, to obtain the temperature evolution of the isothermal interior. The interior of a star becomes isothermal for timescales $t \geq 100$ yr, which are required to dissolve temperature gradients by thermal conduction. Unless the initial temperature of the core is chosen too low, the cooling tracks exit the non-isothermal phase and settle at a temperature predicted by the balance of the dominant neutrino emission and the specific heat of the core *at the exit temperature*. The low-density envelope maintains substantial temperature gradients throughout the entire evolution; the temperature drops by about 2 orders of magnitude within this envelope. The isothermal-interior approximation relies further on the fact that the details of the temperature gradients within the envelope are unimportant if we are interested only in the surface temperature T_s . Models of the envelopes predict the scaling $T_s^4 = g_s h(T)$, where g_s is the surface gravity, and h is some function which depends on T , the opacity of crustal material, and its EOS. The fitted formula $T_8 = 1.288(T_{s6}^4/g_{s14})^{0.455}$ [26] is commonly used.

In the isothermal-interior approximation, the parabolic differential equation for the temperature reduces to an ordinary differential equation,

$$C_V \frac{dT}{dt} = -L_\nu(T) - L_\gamma(T_s) + H(T), \quad (4)$$

where L_ν and L_γ are the neutrino and photon luminosities, C_V is the specific heat of the core, and the heating processes, which could be important in the photon cooling era, are neglected, *i.e.*, $H(T) = 0$ (see Refs. [27, 28] for a summary of these processes and their effect on the evolution). The results of integration of Eq. (4) are shown in Fig. 2, where we display the dependence of the (redshifted) surface temperature on time. Each panel of Fig. 2 contains cooling tracks for the same set of four models with central densities 5.1, 10.8, 11.8, 21.0 in units of $10^{14} \text{ g cm}^{-3}$. The cooling tracks for the purely hadronic model (solid lines) are the same in all four panels. The panels differ in the values of micro-physics parameters, which characterize the pairing pattern in quark matter. Specifically, the two panels in the left column correspond to the case where the blue-quark pairing is negligible (*i.e.*, the pairing is on a scale much smaller than the smallest energy scale involved, typically the core temperature). The two panels in the right column correspond to the case where the gap for blue quarks is large, $\Delta_b = 0.1$ MeV. The panels in the upper and lower rows are distinguished by the value of the ζ parameter. [We use the values $\zeta = 0.9$ (upper row) and $\zeta = 1.1$ (lower row)]. It can be seen that (i) the neutrino-cooling is slow for hadronic stars and becomes increasingly fast with an increase of the size of the quark core, in those scenarios where there are unpaired quarks or gapless excitations in the superconducting quark phase. The temperature scatter of the

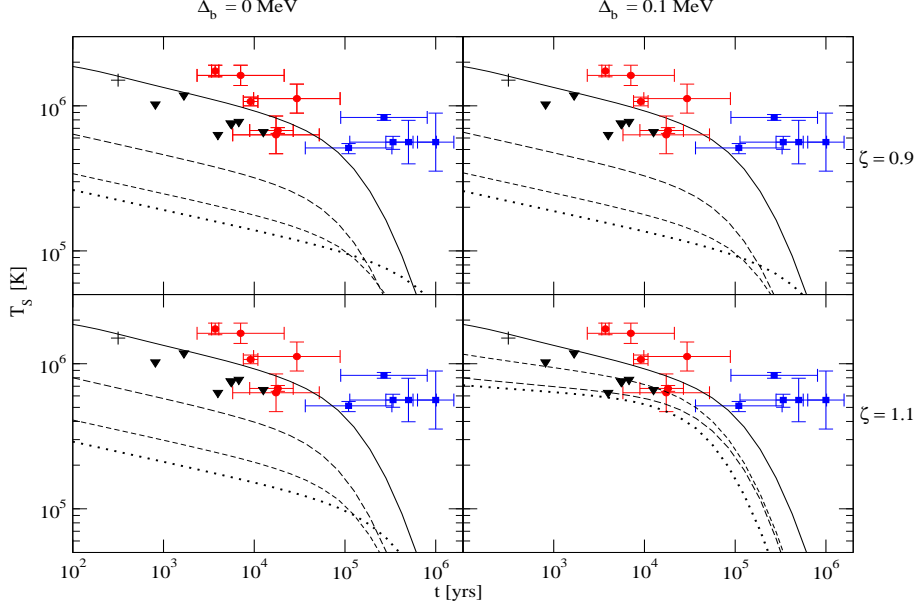


Fig. 2. Time evolution of the surface temperature of four models with central densities 5.1 (solid line), 10.8 (long-dashed line), 11.8 (short-dashed line), 21.0 (dotted line) given in units of $10^{14} \text{ g cm}^{-3}$. For the observational data see Ref. [11]. The upper two panels correspond to cooling when the red-green condensate has $\zeta = 0.9$, i.e., is not fully gapped; the lower panels correspond to $\zeta = 1.1$, i.e., the red-green condensate is fully gapped. The left two panels correspond to evolution with negligible blue-quark pairing ($\Delta_b = 0$); the right two panels show the evolution for large blue pairing $\Delta_b = 0.1 \text{ MeV}$.

cooling curves in the neutrino cooling era is significant and can explain the observed variations in the surface temperature data of same age neutron stars. (ii) If quarks of all colors have gapped Fermi surfaces, the neutrino cooling shuts off early, below the pairing temperature of blue quarks; in this case, the temperature spread of the cooling curves is not as significant as in the fast cooling scenarios. (iii) As the stars evolve into the photon cooling stage the temperature distribution is inverted, *i.e.*, those stars that were cooler in the neutrino-cooling era are hotter during the photon cooling stage.

4. Perspectives

The physics of massive compact stars poses a number of interrelated questions/challenges. The first issue is the EOS of matter, including the quark degrees of freedom and their color superconductivity. The strangeness degrees of freedom including hypernuclear matter and three-flavor quark matter need to be further explored building, e.g., upon the work of Ref. [14]. The equilibrium and stability of massive compact objects, constructed from these EOSs, should be studied including rapid rotations and oscillations. Secondly, we need a better understanding of the weak interaction rates in quark and (hyper)nuclear matter, which are required input in cooling simulations of compact stars. Thirdly, the transport coefficients of dense color superconducting quark matter, such as the thermal conductivity, are needed for modelling an array of phenomena, which include thermal evolution, magnetic evolution, r -modes etc.

Acknowledgements

I would like to thank Luca Bonanno and Daniel Hess for the collaboration on the physics described in this lecture. I would like to thank Mark Alford, Xu-Guang Huang, Dirk H. Rischke and Harmen Warringa for useful discussions. This work was in part supported by the Deutsche Forschungsgemeinschaft (Grant SE 1836/1-2)

REFERENCES

- [1] Weber, F., *Pulsars as astrophysical laboratories for nuclear and particle physics*, Bristol, U.K. : Institute of Physics, 1999.
- [2] A. Sedrakian, Prog. Part. Nucl. Phys. **58**, 168 (2007) [arXiv:nucl-th/0601086].
- [3] P. B. Demorest, T. Pennucci, S. M. Ransom, M. S. E. Roberts and J. W. T. Hessels, Nature **467**, 1081 (2010).
- [4] D. G. Yakovlev, O. Y. Gnedin, A. D. Kaminker and A. Y. Potekhin, AIP Conf. Proc. **983**, 379 (2008) [arXiv:0710.2047 [astro-ph]].
- [5] D. Page, U. Geppert and F. Weber, Nucl. Phys. A **777**, 497 (2006) [arXiv:astro-ph/0508056].
- [6] C. O. Heinke and W. C. G. Ho, Astrophys. J. **719**, L167 (2010) [arXiv:1007.4719 [astro-ph.HE]].
- [7] P. S. Shternin, D. G. Yakovlev, C. O. Heinke, W. C. G. Ho and D. J. Patnaude, Mon. Not. Roy. Astron. Soc. **412**, L108 (2011) [arXiv:1012.0045 [astro-ph.SR]].
- [8] D. Page, M. Prakash, J. M. Lattimer and A. Steiner, Phys. Rev. Lett. **85**, 2048 (2000) [arXiv:hep-ph/0005094].

- [9] M. Alford, P. Jotwani, C. Kouvaris, J. Kundu and K. Rajagopal, *Phys. Rev. D* **71**, 114011 (2005) [arXiv:astro-ph/0411560].
- [10] R. Anglani, G. Nardulli, M. Ruggieri and M. Mannarelli, *Phys. Rev. D* **74**, 074005 (2006) [arXiv:hep-ph/0607341].
- [11] D. Hess and A. Sedrakian, *Phys. Rev. D* **84**, 063015 (2011) [arXiv:1104.1706 [astro-ph.HE]].
- [12] M. G. Alford, A. Schmitt, K. Rajagopal and T. Schafer, *Rev. Mod. Phys.* **80**, 1455 (2008) [arXiv:0709.4635 [hep-ph]].
- [13] Q. Wang, *Prog. Phys.* **30**, 173 (2010) [arXiv:0912.2485 [nucl-th]].
- [14] L. Bonanno and A. Sedrakian, arXiv:1108.0559 [astro-ph.SR].
- [15] N. K. Glendenning and S. A. Moszkowski, *Phys. Rev. Lett.* **67**, 2414 (1991).
- [16] N. K. Glendenning, *Astrophys. J.* **293**, 470 (1985).
- [17] G. A. Lalazissis, J. Konig and P. Ring, *Phys. Rev. C* **55**, 540 (1997) [nucl-th/9607039].
- [18] S. B. Ruester, V. Werth, M. Buballa, I. A. Shovkovy and D. H. Rischke, arXiv:nucl-th/0602018.
- [19] N. D. Ippolito, G. Nardulli and M. Ruggieri, *JHEP* **0704**, 036 (2007) [arXiv:hep-ph/0701113].
- [20] N. Ippolito, M. Ruggieri, D. H. Rischke, A. Sedrakian and F. Weber, *Phys. Rev. D* **77**, 023004 (2008) [arXiv:0710.3874 [astro-ph]].
- [21] B. Knippel and A. Sedrakian, *Phys. Rev. D* **79**, 083007 (2009) [arXiv:0901.4637 [astro-ph.SR]].
- [22] M. G. Alford, J. A. Bowers, J. M. Cheyne and G. A. Cowan, *Phys. Rev. D* **67**, 054018 (2003) [arXiv:hep-ph/0210106].
- [23] M. Buballa, J. Hosek and M. Oertel, *Phys. Rev. Lett.* **90**, 182002 (2003) [arXiv:hep-ph/0204275].
- [24] A. Schmitt, *Phys. Rev. D* **71**, 054016 (2005) [arXiv:nucl-th/0412033].
- [25] P. Jaikumar, C. D. Roberts and A. Sedrakian, *Phys. Rev. C* **73**, 042801(R) (2006) [arXiv:nucl-th/0509093].
- [26] E. H. Gudmundsson, C. J. Pethick, and R. I. Epstein, *Astrophys. J.* **272**, 286 (1983).
- [27] C. Schaab, A. Sedrakian, F. Weber and M. K. Weigel, *Astron. Astrophys.* **346**, 465 (1999) [arXiv:astro-ph/9904127].
- [28] D. Gonzalez and A. Reisenegger, arXiv:1005.5699 [astro-ph.HE].